Investigation of the unsteady flow over a wing under gust excitation

Lancelot, Paul; Sodja, Jurij; De Breuker, Roeland

Publication date
2017

Document Version
Accepted author manuscript

Published in
17th International Forum on Aeroelasticity and Structural Dynamics, IFASD 2017

Citation (APA)
Lancelot, P., Sodja, J., & De Breuker, R. (2017). Investigation of the unsteady flow over a wing under gust excitation. In *17th International Forum on Aeroelasticity and Structural Dynamics, IFASD 2017* (Vol. 2017-June). Article IFASD-2017-185 International Forum on Aeroelasticity and Structural Dynamics (IFASD).

International Forum on Aeroelasticity and Structural Dynamics

IFASD 2017

25-28 June 2017, Como - Italy

INVESTIGATION OF THE UNSTEADY FLOW OVER A WING UNDER GUST EXCITATION

Paul Lancelot[1], Jurij Sodja[1], and Roeland De Breuker[1]

[1] Faculty of Aerospace Engineering
Delft University of Technology
P.M.G.J.Lancelot@tudelft.nl, j.sodja@tudelft.nl, r.debreuker@tudelft.nl

Keywords: Gust generator, unsteady aerodynamics, unsteady loads.

Abstract: A detailed performance investigation of the gust generator built for the Open Jet Facility wind tunnel at TU Delft is summarised in this paper. The influence of various parameters such as reduced frequency, measurement location, and excitation amplitude on the generated gust profile was quantified. In addition, unsteady lift measurements were performed using a rigid wing exposed to various gust profiles. In addition, unsteady incremental lift was compared with the DLM method which showed good agreement.

1 INTRODUCTION

Gust encounter is among the most critical load cases an aircraft can experience during service life. The increasing aspect ratio of modern commercial aircraft wings and reducing structural weight generally result in an increased sensitivity of the wing to gust loads. Gust loads mainly come from atmospheric condition [1] and can be represented as in Figure 1. Researchers have been looking for solutions to reduce structural stresses at the wing root caused by gust encounters either by using passive (e.g. aeroelastic composite tailoring) or active methods (e.g. using control surfaces). Reducing loads reduces airframe weight and hence operational cost of the aircraft. In order to ease the development of these methods, many computational techniques of different fidelity levels have been developed to evaluate the structural response to gust loads. Nonetheless, the unsteady nature of a gust flow and strong coupling between resulting aerodynamic loads and structural deformations make the modelling of a pertinent dynamic response a challenging task. Hence code validation through wind tunnel experiment is necessary. In order to perform such test in a wind tunnel, a gust generator is required.

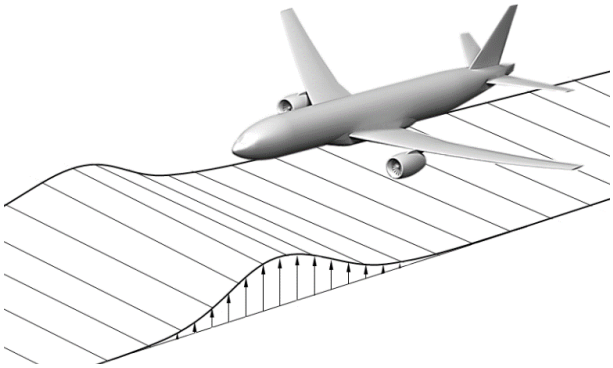

Figure 1: Illustration of a vertical gust hitting an aircraft in flight.

Few research institutes and universities have been operating gust generators for the purpose of their own research. Gust response experiments have been carried out, either on a clamped wing [3], [4], on an aeroelastic apparatus [5] or on a wing mounted on a free flying aircraft model [6], [7].

Research Institute/University	Year	Top speed	Wind tunnel cross section
NASA (USA) [1]	1966	Mach 1.2	Square 4.9×4.9m^2
MIT (USA) [2]	1974	37m/s	Elliptical 2.13×3.32m^2
Duke University (USA) [3]	1996	25m/s	Rectangular 0.7×0.53m^2
Virginia Tech (USA) [4]	2004	15m/s	Square 2.15×2.15m^2
TSAGI (Russia) [5]	2005	30m/s	Elliptical 4.0×2.33m^2
TSAGI (Russia) [5]	2005	120m/s	Circular 7m diameter
University of Maryland (USA) [6]	2008	N/A	N/A
Politecnico di Milano (Italy) [7]	2008	30m/s	Rectangular 1.0×1.5m^2
University of Colorado,(USA) [8]	2009	20m/s	Square 0.34×0.34 m^2
DLR (Germany) [9]	2010	Mach .75	Square 1.0×1.0m^2
ONERA (France) [10]	2011	Mach .73	Rectangular 0.76×0.8m^2
Beihang University (China) [11]	2012	24m/s	Square 3×3 m^2
Cal Poly Pomona (USA)	2013	61m/s	Rectangular 1.0×0.71m^2
Delft University of Technology [12]	2015	29 m/s	Octagonal 2.85×2.85 m^2
Cranfield University (England) [13]	2015	14.5m/s	Elliptical 1.52×1.14m^2
ARA (England) [14]	2015	Mach .85	Rectangular 2.74×2.44 m^2
Politecnico di Milano (Italy)[15]	2016	55m/s	Rectangular 4.0×3.84 m^2
University of Bristol (England)[16]	2016	60m/s	Octagonal 2.1×1.5 m^2
University of Bristol (England)[17]	2016	20 m/s	Circular 1.1m diameter
Mitsui engineering (Japan) [18]	N/A	20m/s	N/A
JAXA (Japan) [19]	N/A	Transonic	N/A

Table 1: Summary of existing gust generator installations around the world. If the top speed achieved during gust experiments isn't available, the maximum speed of the wind tunnel is written instead.

A gust generator was built for the Open Jet Facility wind tunnel at the Delft University of Technology. The wind tunnel features a test section of 2.85 × 2.85 m^2 and can achieve flow speeds of up to 35 m/s. This paper presents further investigation of the unsteady flow induced by the gust generator and the unsteady aerodynamic behaviour of a wing hit by a gust. Moreover, the presented activities present an important stepping stone towards an aeroelastic experiment investigating passive and active load alleviation concepts on a flexible wing such as composite tailoring or control surface scheduling being developed at Delft University of Technology.

2 EXPERIMENTAL SETUP

The experiment presented here investigates the effect of the gust encounter by a wing on the aerodynamic loads. The experimental setup therefore consists of three main components: the gust generator, the particle image velocimetry (PIV) and the load measurement system experiment. The gust generator itself has already been presented in detail in [12]. Hence it will not be discussed in further detail here. Nevertheless, the PIV and load measurement

system are presented in more detail in Sec. 2.1 and 2.2 respectively. Finally, the measurement procedure is discussed in Sec. 2.3.

2.1 PIV setup

PIV was performed to investigate the unsteady flow downstream the gust generator. A good description of PIV functioning and application is provided by [20].

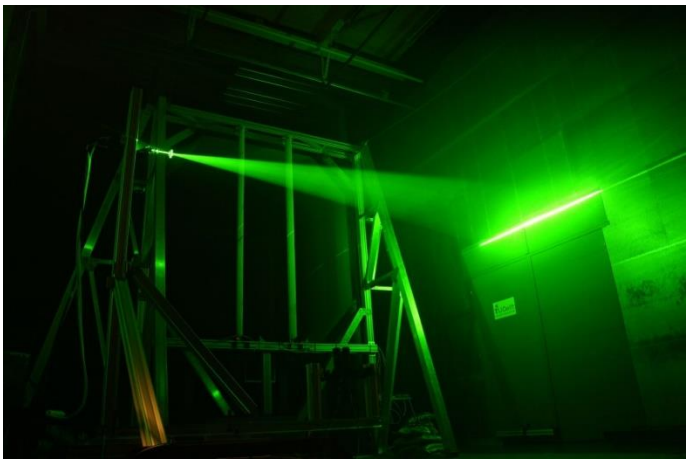

Figure 2: PIV light sheet/measurement plane

A commercial system provided by LaVision was used in order to perform the PIV measurements. Davis 8.3 was used to acquire and process the frames captured by a pair of high-resolution cameras (Imager Pro LX 16M) and to control the programable time unit (PTU v9). PTU v9 was used to synchronise the laser pulse with the camera exposition. The PTU v9 was also configured to accept the trigger signal generated by the gust generator control system in order to facilitate phase-locked PIV imaging. This way the evolution of the high frequency gusts could be obtained despite the low sampling frequency of the PIV system. A double pulsed Nd:YAG laser (Evergreen 200) was used as the light source. The PIV setup along with the calibration plate for the cameras is shown in Figure 3.

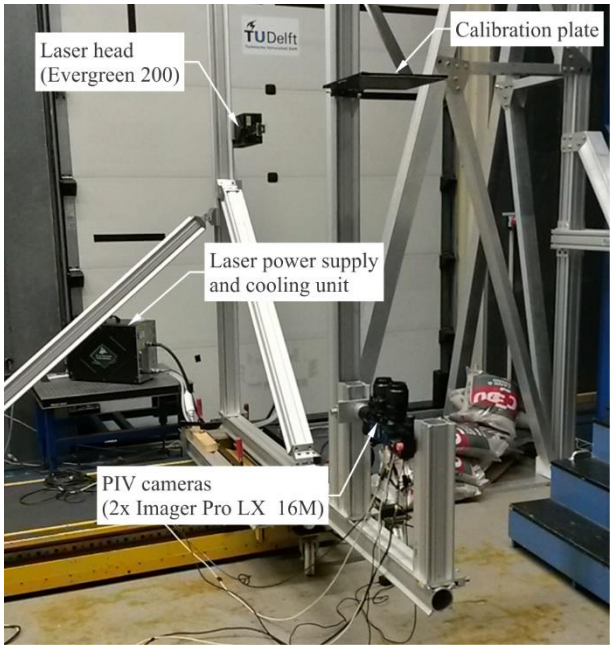

Figure 3: PIV setup

The two cameras were configured in a side-by-side configuration in order to increase the size of the viewing field in the measurement plane (up to 30 x 35 cm^2). Consequently, only a 2D flow field in the measurement plane could be recovered. As shown in Figure 4, the two areas overlap, to ease the match between the two sets of pictures generated. The measurement plane is effectively defined by the light sheet created by the laser as shown in Figure 2, whereas the actual stream wise measurement locations are indicated in Figure 5.

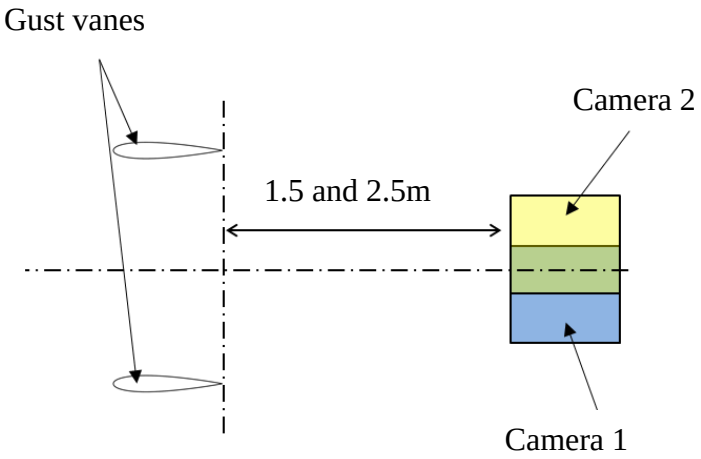

Figure 4: Schematic of the two areas covered by the cameras. Note that the drawing is not at scale.

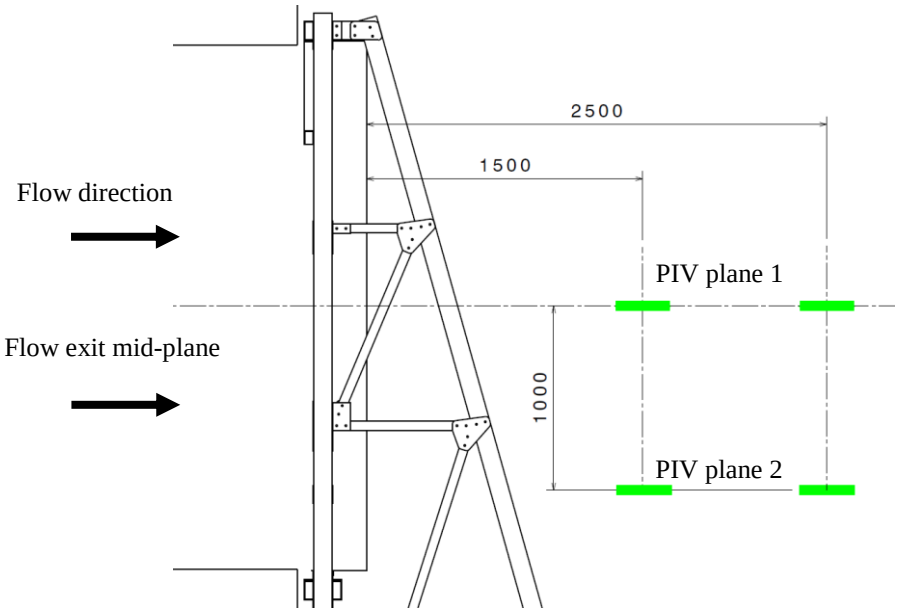

Figure 5: Schematic of the different measurement locations behind the gust generator. The green segments indicate the observation "windows" for the PIV.

2.2 Load measurement

Unsteady loads were measured by mounting a test wing on a six-component balance as shown in Figure 6. The balance properties are summarised in Table 2 whereas the axis definitions and sign conventions are defined in Figure 7. It is important to point out that the balance reference point BC is located 168.5mm below the wing mount plate. The location of the BC has to be accounted for in the calculation of the wing root moments.

A splitter plate was installed at the root of the test wing in order to provide a clean airflow to the test wing and to shield the measurement equipment. The wing has a symmetric airfoil NACA 0012. It is 1m in span and 0.2m in chord. The wing was build out of carbon fibre prepreg with quasi-isotropic layup. The wing was designed to withstand aerodynamic loads at airstream velocities of up to $120\mathrm{m/s}$, hence the wing behaved as if rigid during this particular experiment with the airflow velocities not exceeding $30\mathrm{m/s}$. The whole experiment was mounted on a support table. Therewith the position and the attitude of the wing with respect to the airflow could be precisely controlled.

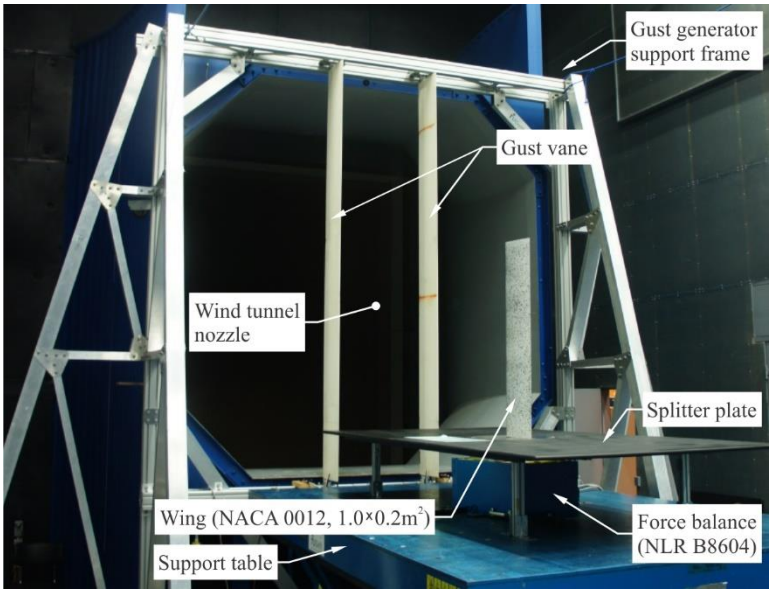

Figure 6: Wing model mounted on a load balance behind the gust generator

Component	Range	Accuracy
F_x	$\pm 250\mathrm{N}$	0.06%†
F_y	$\pm 500\mathrm{N}$	0.23%
F_z	$\pm 500\mathrm{N}$	0.16%
M_x	$\pm 500\mathrm{Nm}$	0.05%
M_y	$\pm 250\mathrm{Nm}$	0.05%
M_z	$\pm 50\mathrm{Nm}$	0.25%

†Relative to the full-scale range

Table 2: Load balance properties

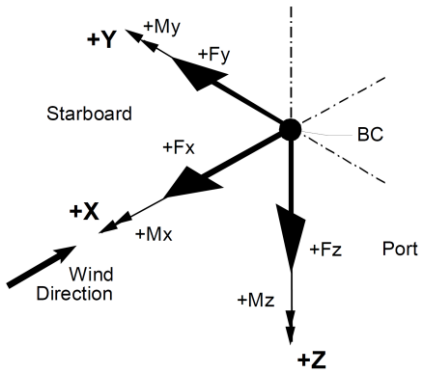

Figure 7: Balance axis system and sign convention

2.3 Measurement procedure

The experiment was performed in two stages. First the gust flow was measured using PIV in the absence of the test wing in order to obtain a clean gust profile over a range of airstream velocities, vane actuation amplitudes and frequencies and vertical planes. Gust characterisation was performed based on these measurements.

In the second stage a wing was mounted in the flow and the corresponding gust response in terms of unsteady loads were measured. Hence, nonlinear unsteady aerodynamic effects such as dynamic flow separation could be observed by correlating flow and load measurements. These tests were performed at a range of reduced frequencies, wing incidence angles and free stream velocities. The reduced frequency was varied from 0.05 to 0.2, the wing incidence angle was set to 0deg, 4deg and 8deg and the free stream velocity was set to 15 m/s, 23 m/s and 29 m/s. Finally, the gust vanes were deflected with a maximum amplitude of 5deg, 10deg and 15deg. For both types of measurement, the reduce frequency is computed from the gust vanes half chord length (15 cm).

3 RESULTS AND DISCUSSION

During the wind tunnel campaign a vast amount of experimental data was collected. Hence, only the most interesting findings and observations are presented here. First, the PIV measurements are discussed, followed by the discussion of the obtained unsteady aerodynamic loads.

3.1 PIV measurements

PIV measurements for both sinusoidal and 1-COS gust are presented in this section. As already pointed out in Sec. 2.3, the measurements were completed at several locations in the test chamber at various gust vane actuation amplitudes and frequencies.

Time signal of the measured sinusoidal gusts are shown in Figure 8a. The airstream velocity and the gust vane actuation amplitude were kept constant at 15m/s and ±10deg while the gust reduced frequency was changed from 0.05 to 0.1 and 0.2. The time axis is shown in terms of collected sample points rather than actual time in order to ease the comparison between the measurements at different reduced frequencies. The measurements show that clean and well defined sinusoidal gusts have been produced at all reduced frequencies.

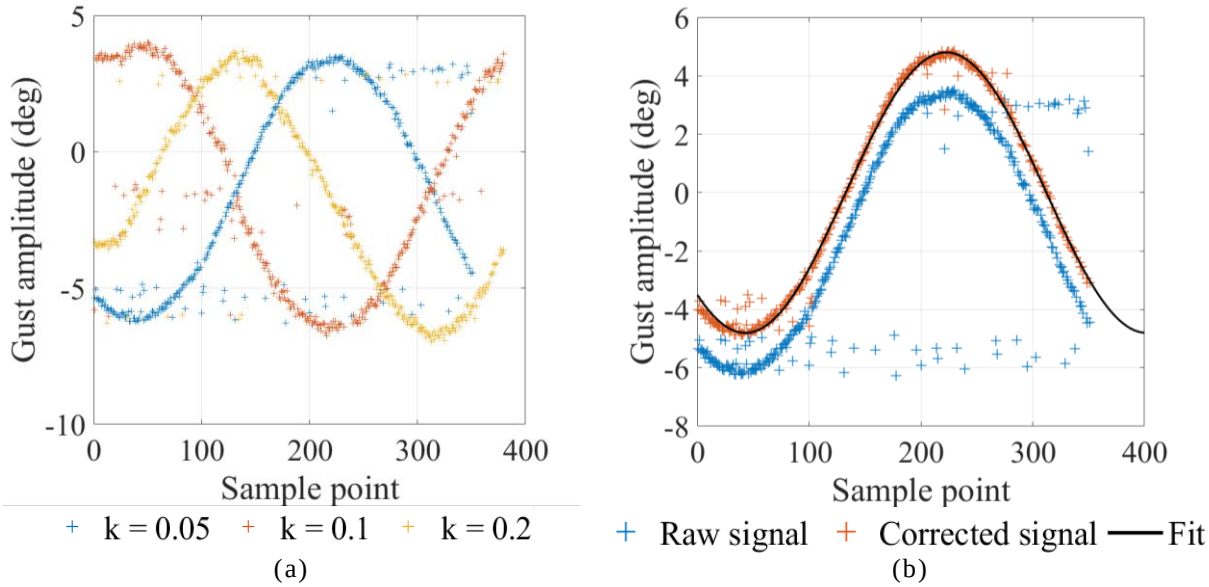

Figure 8: Sinusoidal gust: (a) at reduced frequencies of 0.05, 0.1 and 0.2, and (b) an example of post-processed signal

Figure 8b shows the post-processing methodology used to extract the gust amplitudes shown later in the report. First, the data was filtered in order to remove the failed measurements which can be seen as stray points clustered primarily around the positive and the negative

value of the induced gust amplitude. These measurements are due to the PIV system occasionally misfiring upon the trigger signal. This issue was mitigated primarily by conditioning the trigger signal and performing several measurements at every phase angle of the gust. Next, the mean gust amplitude was removed and a sine function of the corresponding frequency was fitted to the measurements. One can observe that the raw signal shown in Figure 8b has an offset. This is due to a misalignment of the calibration plate for the PIV. This error is removed by the process enunciated above.

1-COS gust were also captured, as shown below on Figure 9. As for the sine wave gusts, the shape is well defined and match the prescribed 1-COS profile.

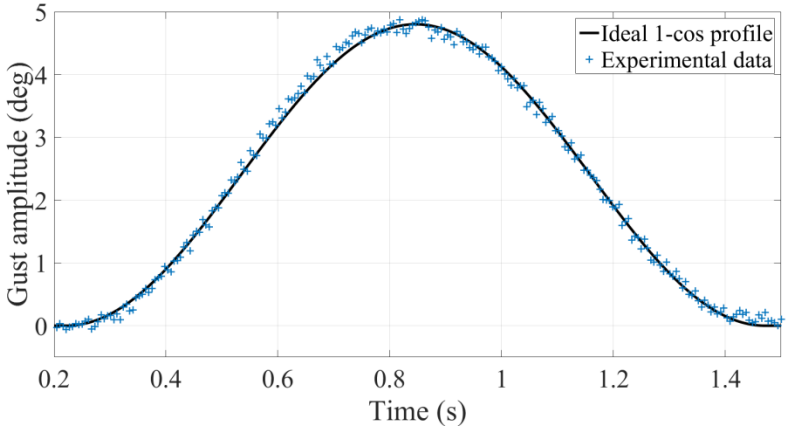

Figure 9: 1-COS gust amplitude experimental results compared with an ideal signal. k = 0.05 and δ =10deg.

On Figure 10 is shown the gust amplitude as respect of time and the transverse direction (perpendicular to main flow direction, see Figure 4). Here, only the results from camera 1 are shown and at the transverse direction = 0mm is the centerline of test the setup. This demonstrates a relatively uniform flow between the gust vanes, which is ideal for wing model experiencing large deflections.

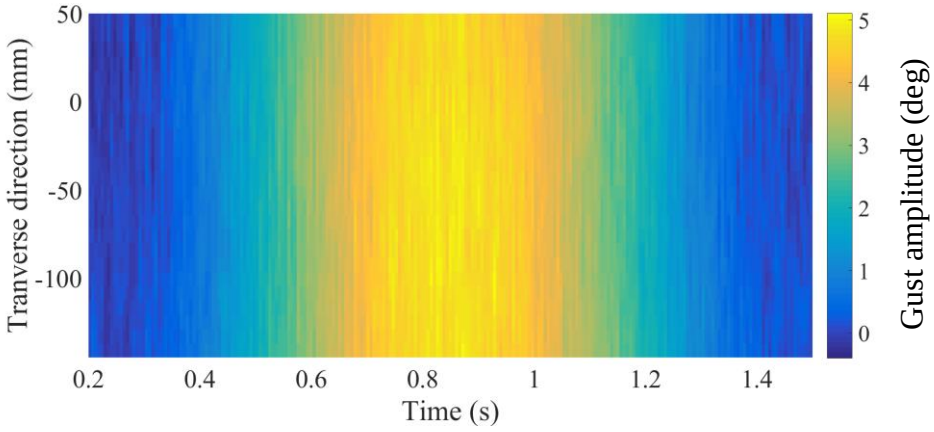

Figure 10: 1-COS gust amplitude measured in time and along the transverse direction. k = 0.05 and δ =10deg.

A synthesis of the measurements taken on “plane 1” at 1.5 and 2.5 m downstream of the gust generator is presented in Figure 11. It can be observed that the gust amplitude scales with the gust vane actuation amplitude. The effects of the reduced frequency vary with the measurement location, but overall remain limited.

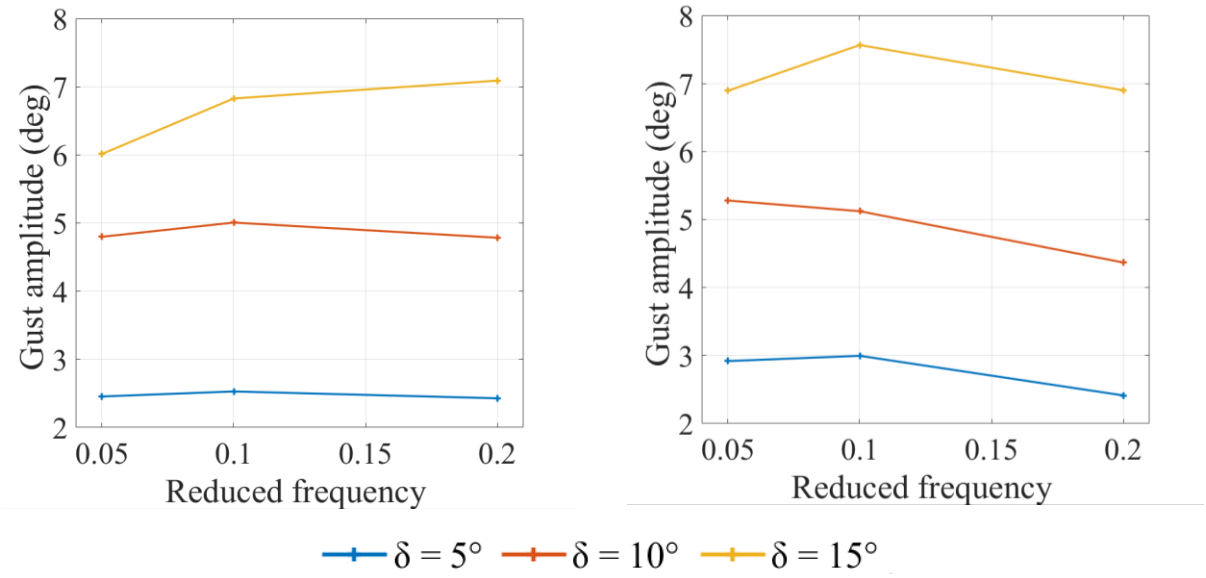

(a) (b)

Figure 11: 1-COS gust amplitude as a function of reduced frequency measured (a) 1.5m, and (b) 2.5m downstream of the gust generator

Additional measurements were also performed on horizontal planes 2, 1.5 m downstream of the gust generator in order to investigate vertical variation of the induced gust flow field. The precise location of the planes 1 and 2 is indicated in Figure 5. The results shown in Figure 12a, correspond to the gust vane deflection of 10 degrees and free stream velocity of 15 m/s.

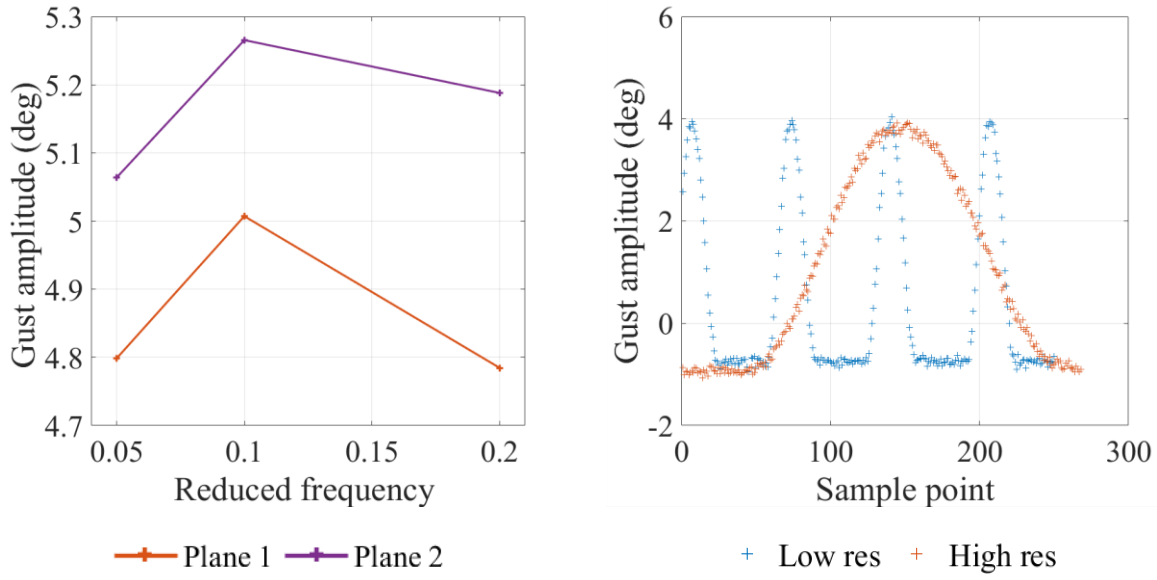

(a) (b)

Figure 12: 1-COS gust, (a) amplitude as a function of reduced frequency, and (b) gust amplitude resolution

A 10% variation in gust amplitude between the two measurement planes is observed. On the other hand, the dependency to the reduce frequency exhibit similar trend. Overall, it can be said that the gust amplitude is relatively consistent in space. Different time resolutions were also tried regarding the PIV data acquisition (35 and 200 points/cycle) as exhibit on Figure 12b and give similar maximum amplitude.

3.2 Force balance results

Results obtained using the load balances are discussed in this section. The test wing was subjected to a sine and 1-COS gust and a parametric study was performed by varying the gust vane amplitude (δ = 5, 10 and 15 degrees), reduced frequency (k = 0.05, 0.1 and 0.2), the flow speed (U = 15 m/s, 23 m/s and 29 m/s) and the initial angle of attack (α = 0, 4 and 8 degrees). The wing was located 1.5 m downstream of the gust generator. Figure 13 shows the amplitude of the unsteady lift coefficient due to a sine wave gust.

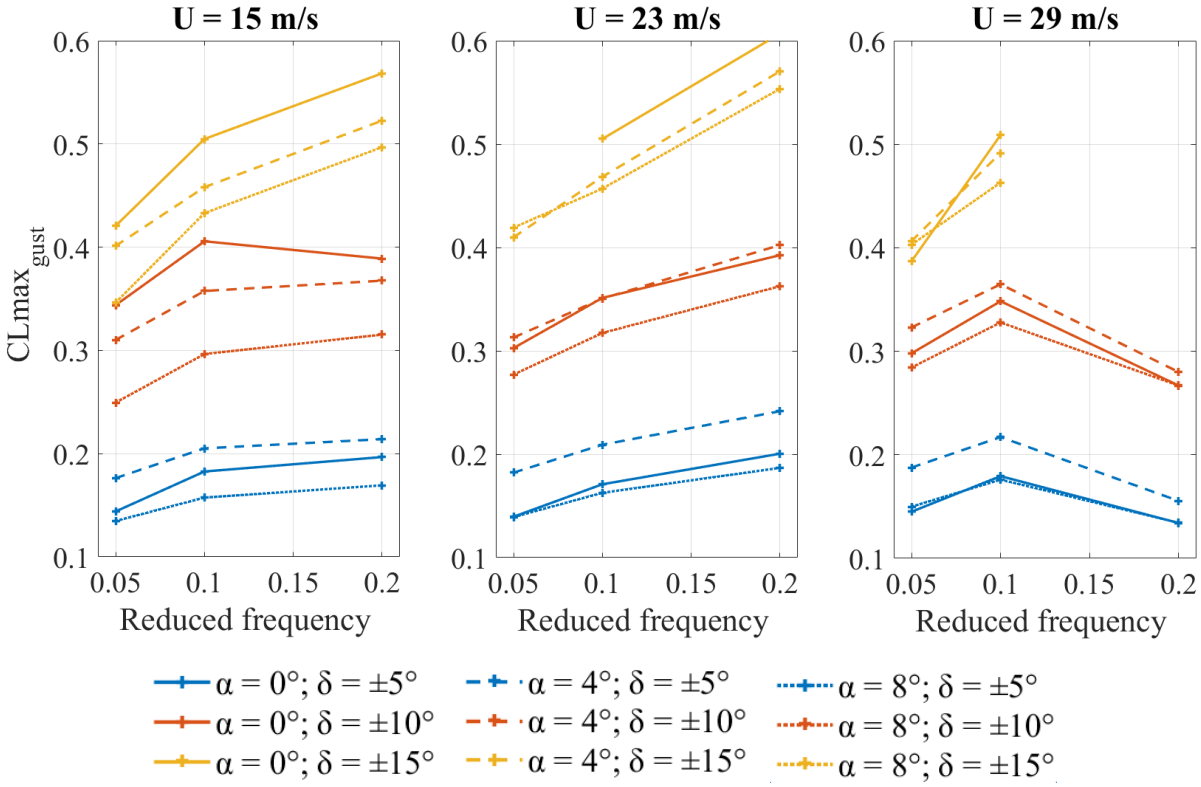

Figure 13: $CLmax_{gust}$ as a function of reduced frequency, geometric angle of attack, and gust vane amplitude measured at $U = 15\text{m/s}$, $U = 23\text{m/s}$ and $U = 29\text{m/s}$ for a SINE gust

It can be observed that overall, $CLmax_{Gust}$ is increased with increasing reduced frequency. This indicates a stronger dependency of the gust amplitude on reduced frequency than initially suggested by the PIV results. Indeed, for constant gust amplitude, the wing response should normally decline with an increase of k. An exception to otherwise consistent behaviour can be observed at 29 m/s, where $CLmax_{Gust}$ drops for k = 0.2. In general, similar behaviour in terms of overall trend without the aforementioned exception was also observed in the response due to the 1-COS gust shown in Figure 14. Hence, the exception observed at k = 0.2 at U = 29m/s cannot be attributed to the gust itself.

The measurements consistently indicate that a lower $CLmax_{Gust}$ was obtained at α = 8deg relative to the $CLmax_{Gust}$ obtained at $\alpha = 0$deg and 4deg at lower free stream velocities, namely at U = 15 m/s and 23 m/s. However, at U = 29 m/s the observed difference is much smaller. Such behaviour points to a dynamic stall occurring on the test wing since this effect tends to reduce at higher speed and therefore higher Reynolds number. Finally, $CLmax_{Gust}$ increases almost linearly with the gust vane deflection and corroborates the PIV results.

Results obtained with a 1-COS gust excitation are shown in Figure 14. Again, the aerodynamic loads are expressed in terms of incremental lift coefficient, $\mathrm{CLmax}_{\mathrm{gust}}$. Analogous conclusions to those pertinent to the SINE gust can be drawn for the 1-COS gust results as well. At $\alpha = 8\mathrm{deg}$ and U = 15m/s and 23 m/s, the lower $CLmax_{gust}$ indicates the onset of dynamic stall. However, the dependency of the $CLmax_{gust}$ on k is less pronounced.

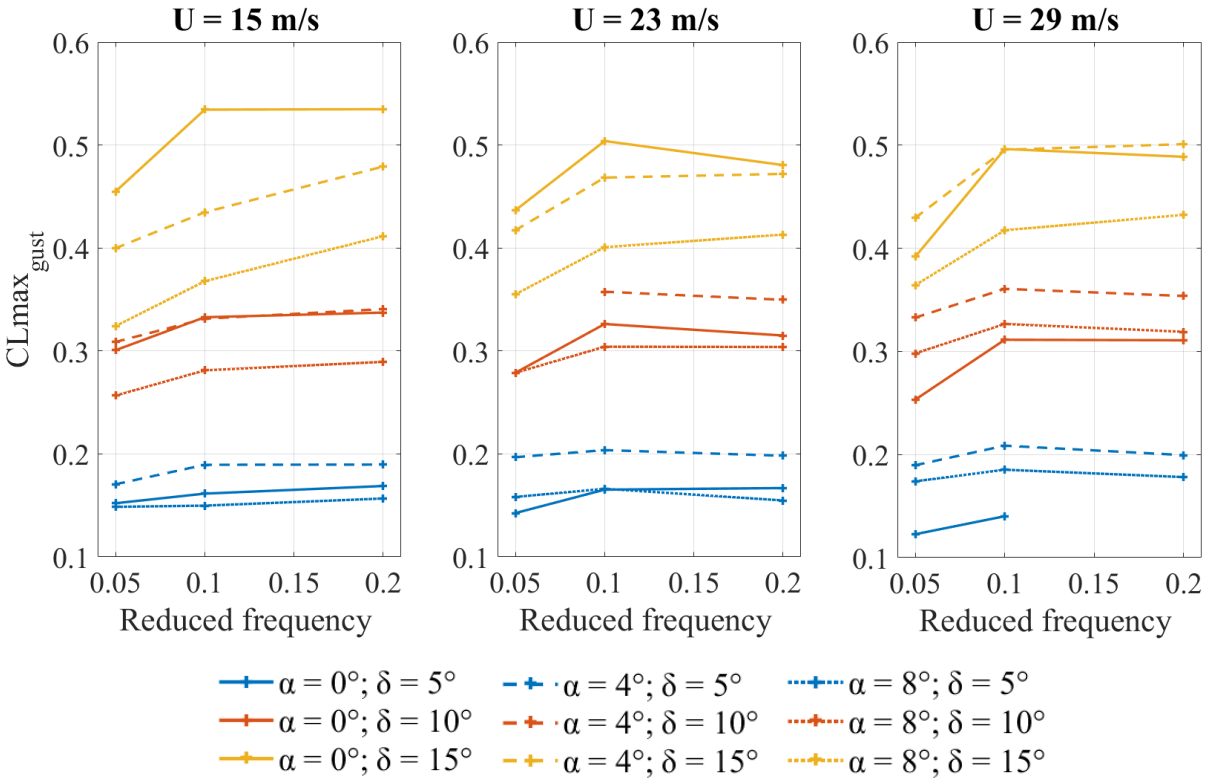

Figure 14: $CLmax_{gust}$ as a function of reduced frequency, geometric angle of attack, and gust vane amplitude measured at $U = 15$ m/s, $U = 23$ m/s and $U = 29$ m/s for a 1-COS gust

Finally, the measured $CLmax_{gust}$ are compared with numerical predictions as shown in Figure 15a. Numerical results were obtained with the Doublet Lattice Method (DLM) solution implemented into the Solution 146 of MSC.NASTRAN [21]. Only the flow speed of 15 m/s was considered in order to match the gust amplitudes obtained with the PIV as displayed Figure 11a. Moreover, only the incremental lift due to 1-COS gust was considered. Hence the static angle of attack was set to 0deg. Good agreement between experimental and numerical results was achieve, with a mean difference of 8.7% across the 9 data points.

Moreover, steady lift coefficient (*CL*) were also measured and compared to the numerical results for various flow speed and angles of attack. Results are depicted in Figure 15b. in general, the comparison yields good agreement.

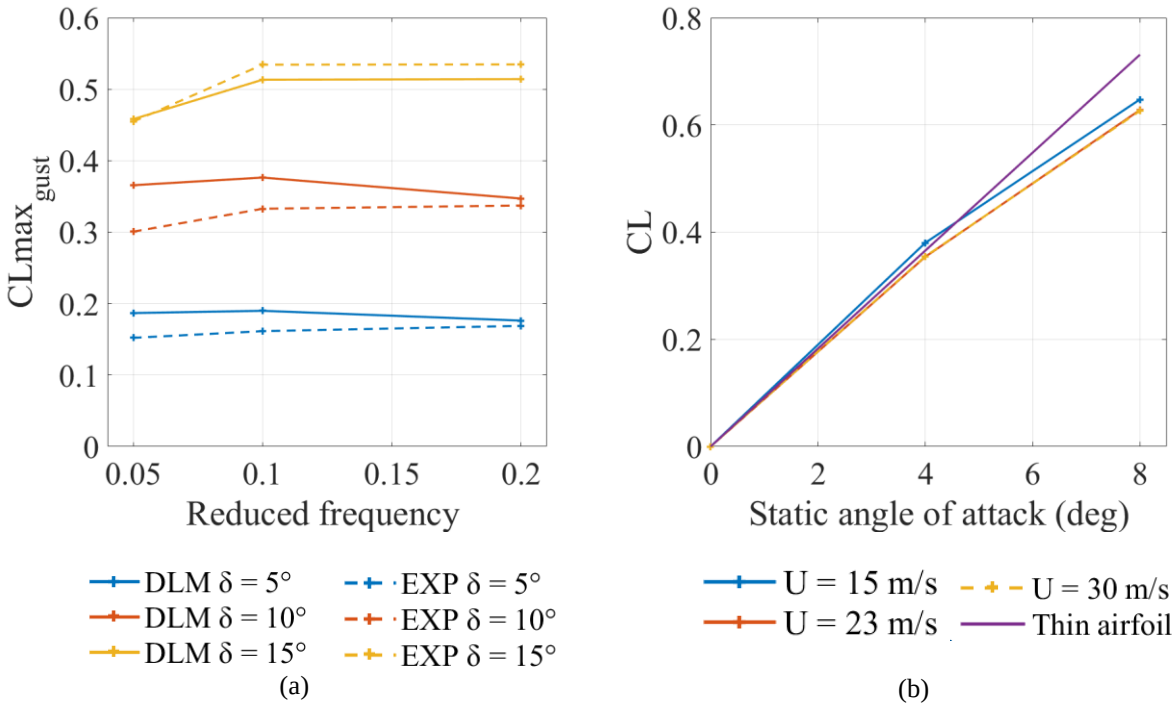

Figure 15: Comparison between numerical and experimental results: (a) gust lift coefficient, and (b) steady lift coefficient

4 CONCLUSIONS

A detailed characterisation of the influence of various parameters such as reduced frequency, measurement location, and excitation amplitude on the generated gust profile has been carried out. In addition, unsteady lift measurements were performed on a rigid wing exposed to various gust profiles.

Both PIV and loads measurements corroborate the almost-linear relation between the gust amplitude and the gust vane deflection. It is also observed that the gust flow is relatively consistent in space. The effect of the reduced frequency remains difficult to assess as some discrepancy exist between the PIV and the force balance measurements.

Nonetheless, the unsteady incremental lift was match with DLM method with a limited error.

In conclusion, a good overview of the gust characteristic produced inside the OJF was achieved which also confirmed that gust of high repeatability can be generated. This open the door to the experiments featuring larger and more complex wind tunnel models for which unsteady loads can now be accurately estimated.

Finally, additional results collected during the experimental campaign will also be exploited to refine our current study with drag and moments values.

5 ACKNOWLEDGMENT

The authors deeply appreciate the help and support from Dr. Daniele Ragni and Nico van Beek at setting up the PIV and load measurements in the wind tunnel.

6 REFERENCES

[1] W. H. Reed, "Aeroelasticity matters: Some reflections on two decades of testing in the NASA Langley transonic dynamics tunnel," presented at the Intern. Symp. on Aeroelasticity, Nuremberg, Germany, 1981.

[2] N. D. Ham, P. H. Bauer, and T. L. Lawrence, "Wind Tunnel Generation of Sinusoidal Lateral and Longitudinal Gusts by Circulation of Twin Parallel Airfoils," Aug. 1974.

[3] D. M. Tang, P. G. A. Cizmas, and E. H. Dowell, "Experiments and analysis for a gust generator in a wind tunnel," *J. Aircr.*, vol. 33, no. 1, pp. 139–148, 1996.

[4] D. Grissom and W. Devenport, "Development and Testing of a Deterministic Disturbance Generator," in *10th AIAA/CEAS Aeroacoustics Conference*, 2004.

[5] S. Kuzmina, F. Ishmuratov, M. Zichenkov, and V. Chedrik, "Analytical-Experimental Study on Using Different Control Surfaces to Alleviate Dynamic Loads," in *47th AIAA/ASME/ASCE/AHS/ASC Structures, Structural Dynamics, and Materials Conference*, 2005.

[6] S. Koushik and F. Schmitz, "A New Experimental Approach to Study Helicopter Blade-Vortex Interaction Noise," in *14th AIAA/CEAS Aeroacoustics Conference (29th AIAA Aeroacoustics Conference)*, 2007.

[7] S. Ricci and A. Scotti, "Wind Tunnel Testing of an Active Controlled Wing Under Gust Excitation," in *49th AIAA/ASME/ASCE/AHS/ASC Structures, Structural Dynamics, and Materials Conference*, 2008.

[8] J. Roadman and K. Mohseni, "Gust Characterization and Generation for Wind Tunnel Testing of Micro Aerial Vehicles," in *47th AIAA Aerospace Sciences Meeting including The New Horizons Forum and Aerospace Exposition*, 2009.

[9] J. Neumann and H. Mai, "Gust response: Simulation of an aeroelastic experiment by a fluid–structure interaction method," *J. Fluids Struct.*, vol. 38, pp. 290–302, Apr. 2013.

[10] A. Lepage, Y. Amosse, D. Le Bihan, C. Poussot-Vassal, V. Brion, and E. Rantet, "A complete experimental investigation of gust load : from Generation to active control," presented at the International Forum on Aeroelasticity and Structural Dynamics, Saint Petersburg, 2015.

[11] Z. Wu, L. Chen, and C. Yang, "Study on gust alleviation control and wind tunnel test," *Sci. China Technol. Sci.*, vol. 56, no. 3, pp. 762–771, Jan. 2013.

[12] Paul Lancelot , Jurij Sodja, Noud Werter and Roeland De Breuker, "Design and testing of a low subsonic wind tunnel gust generator," *Adv. Aircr. Spacecr. Sci.*, vol. 4, no. 1, Feb. 2017.

[13] A. J. Saddington, M. V. Finnis, and K. Knowles, "The characterisation of a gust generator for aerodynamic testing," *Proc. Inst. Mech. Eng. Part G J. Aerosp. Eng.*, p. 0954410014548237, Sep. 2014.

[14] N. J. Allen and M. Quinn, "Development of a Transonic Gust Rig for Simulation of Vertical Gusts on Half-models," in *31st AIAA Aerodynamic Measurement Technology and Ground Testing Conference*, 2015.

[15] S.Ricci, S.Adden, C.Servadio, M.Karpel and J.Cooper, "WIND TUNNEL EXPERIMENTAL VALIDATION OF FUTURE GREEN REGIONAL A/C GUST LOAD ALLEVIATION CONTROL SYSTEM," presented at the IFASD, Saint Petersburg, 2015.

[16] K. T. Wood, R. C. Cheung, T. S. Richardson, J. E. Cooper, O. Darbyshire, and C. Warsop, "A New Gust Generator for a Low Speed Wind Tunnel: Design and Commissioning," in *55th AIAA Aerospace Sciences Meeting*, American Institute of Aeronautics and Astronautics.

[17] R. C. Cheung, A. Castrichini, and J. E. Cooper, "Testing of Wing-Tip Spring Device for Gust Loads Alleviation," in *58th AIAA/ASCE/AHS/ASC Structures, Structural Dynamics, and Materials Conference*, American Institute of Aeronautics and Astronautics.

[18] "Test fixture - SAN TECHNOLOGIES CO.,LTD." [Online]. Available: http://www-en.santech.co.jp/test-research/test-fixture. [Accessed: 01-Aug-2016].

[19] Saitoh Kenichi, Koike Shunsuke, Suzuki Koichi, "TEST AND ANALYSIS OF A GUST GENERATOR FOR A TRANSONIC WIND-TUNNEL," presented at the IFASD, Saint Petersburg, 2015.

[20] F. Scarano, "Tomographic PIV: principles and practice," *Meas. Sci. Technol.*, vol. 24, no. 1, p. 012001, 2013.

[21] MSC.Software Corporation, *MSC Nastran 2014 Aeroelastic Analysis User's Guide*. 2014.

COPYRIGHT STATEMENT